Effect of oxidation on the gel properties of porcine myofibrillar proteins and their binding abilities with selected flavour compounds

www.reading.ac.uk/centaur

CentAUR

Central Archive at the University of Reading

Reading's research outputs online

1   Effect of oxidation on the gel properties of porcine myofibrillar proteins and their

2   binding abilities with selected flavour compounds

3   Hui Shen[1], J. Stephen Elmore[2], Mouming Zhao[1,3], Weizheng Sun[1,2,3,*]

4   [1]*School of Food Science and Engineering, South China University of Technology,*

5   *Guangzhou 510641, China*

6   [2]*Department of Food and Nutritional Sciences, University of Reading, Whiteknights,*

7   *Reading RG6 6AP, UK*

8   [3]*Overseas Expertise Introduction Center for Discipline Innovation of Food Nutrition*

9   *and Human Health (111 Center), Guangzhou 510641, China*

10

11

12

13   Corresponding author

14   Weizheng Sun, Professor

15   Tel/Fax: +86 20 22236089

16   E-mail: fewzhsun@scut.edu.cn

17 **Abstract**:

18　　In this work, the effect of oxidation induced by hydroxyl radicals on the binding

19　abilities of myofibrillar protein (MP) gels to aldehydes and ketones and their

20　relationship with MP gel properties were investigated. Mild oxidation (0–0.2 mM H_2O_2)

21　could induce partial unfolding of MP, thus slightly increasing the salt solubility of MP

22　and enhancing the hardness of MP gels. MP suffering a higher oxidative attack could

23　undergo a reduction in water-holding capacity, with increased mobility of water in MP

24　gels. Oxidation could make MP gel more disordered. The ability of oxidised MP gels

25　to bind to flavours decreased as the carbon chain length of the flavour compound

26　increased. MP oxidation only significantly affected the binding of MP gels to hexanal,

27　heptanal, and 2-octanone, while other flavour compounds were not affected.

28 **Keywords**: myofibrillar proteins; oxidation; gel properties; flavours release; water

29　mobility

1. Introduction

The formation of protein gels in processed muscle foods is an important functionality that can affect the texture and sensory characteristics of the final meat products. Myofibrillar proteins (MP), as the major proteins in muscle, are excellent gelling agents that are largely responsible for the textural and structural characteristics of meat products (Xiong, Blanchard, Ooizumi, & Ma, 2010).

During meat storage or industrial processing, reactive oxygen species, which include superoxide anions, hydroxyl radicals, peroxyl radicals and lipid oxidation products, play a critical role in the accumulation of oxidative damage in proteins (Zhou, Zhao, Zhao, Sun, & Cui, 2014a). Types of oxidative damage to muscle proteins can include conformational changes, peptide chain scission and formation of amino acid derivatives or aggregates, leading to changes in physicochemical properties of proteins, which in turn alter the functional properties of proteins, such as gelation, emulsification and the capacity to bind flavours (Sun, Zhou, Sun, & Zhao, 2013; Xiong et al., 2010). The gel properties of MP, such as rheological properties, water-holding capacity (WHC), texture and microstructure change under oxidative stress (Xiong, Park, & Ooizumi, 2009).

Food acceptability by consumers is governed to a considerable extent by their organoleptic properties, and mostly by flavour perception (Gierczynski, Guichard, & Laboure, 2011). Volatile flavour release is largely determined by the tendency of volatile compounds to bind to other ingredients (particularly oils and protein) and by food microstructure (Guichard, 2002). As mentioned above, protein oxidation can affect meat products microstructure, especially gel quality. Some reports have evaluated the abilities of oxidised MP at different oxidation levels to bind to flavour compounds (Cao, Zhou, Wang, Sun, & Pan, 2018; Zhou et al., 2014a). Thus far,

55 investigations regarding the binding of oxidised MP gels to flavour compounds are

56 limited. Modifying food microstructure can also control volatile release in foods (Mao,

57 Roos, & Miao, 2014). Among flavours, the impacts of aldehydes and ketones are of

58 particular interest because of their practical contribution in meat and meat products

59 (Guichard, 2002). Therefore, it is necessary to investigate the behaviour of oxidised MP

60 gels in binding to typical odour-active aldehydes and ketones, to establish the

61 mechanism of flavour release in gelatinous meat products.

62 In this work, MP were exposed to a hydroxyl radical-generating system that is

63 commonly involved in meat and meat products. Examination of the accompanying

64 protein structural changes (sulfhydryl [SH] groups, surface hydrophobicity, salt

65 solubility, particle size distribution) with the results of sodium dodecyl sulfate-

66 polyacrylamide gel electrophoresis [SDS-PAGE]) and with gel properties (hardness,

67 WHC, microstructure, low-field nuclear magnetic resonance [LF-NMR] relaxation

68 time) was designed to investigate the influence of oxidative modification on MP and

69 MP gels. The phenomena of oxidised MP gels binding to typical aldehyde and ketone

70 compounds were evaluated using headspace analysis followed by gas chromatography–

71 mass spectrometry. Moreover, selected aldehyde and ketone compounds of various

72 chain lengths were used to evaluate the contributions of molecular structure to the

73 binding phenomena. The relationship between MP gel properties and their binding

74 abilities is discussed.

75 **2. Materials and methods**

76 *2.1. Materials*

77 Fresh porcine muscle (*longissimus dorsi*) was purchased from a local commercial

78 abattoir (Guangzhou, China), where the pigs were slaughtered at approximately 6

79 months of age following standard industrial procedures. Fat and connective tissue were

80　removed before the separation of proteins. Pentanal, hexanal, heptanal, octanal, 2-

81　pentanone, 2-heptanone, 5,5'-dithiobis-(2-nitrobenzoic acid) (DTNB) and piperazine-

82　*N*,*N*-bis(2-ethanesulfonic acid) (PIPES) were purchased from Sigma-Aldrich Chemical

83　Co. (St. Louis, MO); 2-hexanone, 2-octanone, propyl gallate and Trolox C were

84　obtained from Aladdin (Shanghai, China). Bromophenol blue (BPB), thiourea,

85　dithiothreitol and EDTA were obtained from Sinopharm Chemical Reagent Co., Ltd.

86　(Shanghai, China). All other chemicals were of analytical reagent grade at minimum.

87　*2.2. Preparation of MP*

88　　MP were extracted according to the method of Shen, Zhao and Sun (2019), with a

89　slight modification. The pH of the MP suspension (0.1 M NaCl) in the last wash was

90　adjusted to 6.25 before centrifugation (2000 *g*, 15 min, 4 °C). The concentrations of MP

91　were measured by the Biuret method using bovine serum albumin as a standard. The

92　MP pellet was kept on ice and used within 2 days.

93　*2.3. Protein oxidation*

94　　MP were suspended (30 mg/mL) in a 15-mM PIPES buffer containing 0.6 M NaCl

95　(pH 6.25). To oxidise them, MP suspensions were incubated at 4 °C for 24 h, using a

96　hydroxyl radical-generating system. The hydroxyl radicals were produced by a 10-μM

97　$FeCl_3$/100-μM ascorbic acid solution with 1 mM H_2O_2. Oxidation was terminated by

98　adding propyl gallate/Trolox C/EDTA (1 mM each) (Xiong et al., 2009). The fresh MP

99　suspension (30 mg/mL) without any hydroxyl radical-generating system or terminating

100　agent was used as the control. The concentrations of MP in the following measurements

101　were adjusted using a 15 mM PIPES buffer (pH 6.25) containing 0.6 M NaCl.

102　*2.4. Total and reactive SH groups*

103　　Total SH contents were determined with a DTNB method with some modifications

104　(Zhou, Zhao, Su, & Sun, 2014b). For determining the level of total SH groups, 1 mL

105   MP suspension (4 mg/mL) was mixed with 5 mL of 0.086 M Tris-Gly buffer (5 mM

106   EDTA, 8 M urea, 0.6 M NaCl, pH 8.0) and 30 μL of 4 mg/mL DTNB (0.086 M Tris-

107   Gly buffer, 5 mM EDTA, 0.6 NaCl, pH 8.0). After incubation at room temperature (25

108    $\pm$ 1 °C) for 30 min, the absorbance at 412 nm was recorded for the calculation of total

109   SH groups using a molar extinction coefficient of 13,600 M^{-1} cm^{-1}. Reactive SH groups

110   were prepared by incubating the reaction mixture in the absence of urea. The blank was

111   run with 15-mM PIPES buffer (pH 6.25) containing 0.6-M NaCl.

112   *2.5. Surface hydrophobicity*

113   The surface hydrophobicity of the MP was measured by the hydrophobic

114   chromophore BPB method (Chelh, Gatellier, & Santé-Lhoutellier, 2006) with a slight

115   modification. This method can determine the surface hydrophobicity of MP, avoiding

116   the solubilisation step of the myofibrils before the protein hydrophobicity determination.

117   The MP suspension (1 mL, 4 mg/mL) was thoroughly mixed with 100 μL BPB (1

118   mg/mL) and kept at ambient temperature (25 $\pm$ 1 °C) for 10 min before centrifugation

119   (5000 *g*, 15 min, 25 °C). The absorbance of each supernatant (diluted for 10 times) was

120   determined at 595 nm against a PIPES buffer blank. A sample with the same treatments

121   in the absence of MP was used as the control. The index of surface hydrophobicity was

122   expressed as the amount of bound BPB, and it was calculated using the following

123   formula (1):

124   BPB bound (μg) $=100 \times (A_{control} - A_{sample})/A_{control}$ (1)

125   *2.6. Salt solubility and MP turbidity*

126   Salt solubility of MP (10 mg/mL) and turbidity of MP suspensions (1 mg/mL) were

127   determined according to Shen et al. (2019). The salt solubility of MPs was measured

128   after centrifuging (5000 *g*, 25 °C) for 20 min to separate the salt-soluble fractions from

129 the insoluble fractions. The result was expressed as the percentage of initial protein

130 concentration.

131   *2.7. Particle size distributions*

132   Particle size distributions of control and oxidised MP were measured with an

133 integrated-laser light scattering instrument (Mastersizer 2000; Malvern Instruments Co.

134 Ltd., Worcestershire, UK). The relative refractive index and absorption were set as

135 1.414 and 0.001, respectively. $D_{4,3}$ is the mean diameter in volume, and $D_{3,2}$ is the mean

136 diameter in surface, called the 'Sauter diameter'. $D_{v,0.5}$ is the size for which 50% of the

137 sample particles have a lower size and 50% have an upper size. The specific surface

138 areas (square metres per gram) were also recorded.

139 *2.8. Sodium dodecyl sulfate–polyacrylamide gel electrophoresis*

140   Sodium dodecyl sulfate-polyacrylamide gel electrophoresis (SDS-PAGE) was

141 performed on MP according to the method described by Zhou et al. (2014b) with a

142 slight modification. Briefly, the MP suspension (4 mg/mL) was mixed in a 1:1 ratio

143 with 50 mM Tris buffer (8 M urea, 2 M thiourea, 3% (w/v) SDS, 0.05% BPB and 20%

144 (v/v) glycerine, pH 6.8) with or without 75 mM dithiothreitol. The samples were boiled

145 for 4 min before centrifugation (10,000 *g*, 10 min, 25 °C). Next, 9 μL of each MP

146 mixture were injected into each gel, comprising a 12% running gel and a 4% stacking

147 gel. The electrophoresis was operated at a constant current of 25 mA using a Mini-

148 PROTEAN 3 Cell apparatus (Bio-Rad Laboratories, Hercules, CA).

149 *2.9. Gel properties*

150 *2.9.1. Preparation of heat-induced gels*

151   For gelation, the control and oxidised MP (30 mg/mL) were prepared for gel property

152 analyses according to the method of Zhou et al. (2014b). The MP suspensions were

153 heated in a water bath from 25 °C to 72 °C at 1 °C/min increments (kept for 5 min at

154 53 °C and 10 min at 72 °C). After heating, the gels were immediately cooled to room

155 temperature.

2.9.2. Gel hardness and WHC

157 Prior to the hardness measurements, gel samples were allowed to equilibrate at room

158 temperature (25 ± 1°C) for 1 h. The hardness of MP gels was measured using a cylinder

159 measuring probe (P/0.5S, 12.7 mm) attached to TA-XT Plus Texture Analyzer (Stable

160 Micro Systems Ltd., Godalming, UK) at a constant probe speed of 1.0 mm/s at room

161 temperature. The gel hardness was defined as the initial force required to rupture the

162 gels.

163 WHC values for the gels were determined by a centrifugal method (Xia, Kong, Xiong,

164 & Ren, 2010). Briefly, gel samples (3 g) were centrifuged at 4000 *g* for 15 min at room

165 temperature. The WHC (%) was expressed using the final weight as a percentage of the

166 weight before centrifugation (6000 *g*, 15 min, 4 °C).

2.9.3. Microstructure

168 The surface morphologies of control and oxidised MP gels were examined using field

169 emission scanning electron microscopy (FE-SEM, model S-3400N; Hitachi, Japan) at

170 an accelerator voltage of 15 kV. Cubic samples (approximately $3 \times 3 \times 3$ mm) were

171 prepared and snap-frozen in liquid N_2 (Zhou et al., 2014a). Before imaging, freeze-

172 dried gel samples were mounted on a holder with double-sided adhesive tape and

173 sputter-coated with gold (JFC-1200 fine coater; JEOL, Tokyo, Japan). Sample

174 observation and photomicrography were performed at 500× and 2000× magnifications,

175 respectively.

2.9.4. Low-field NMR relaxation time (T_2)

177 Low-field NMR relaxation measurements were performed according to a previous

178 method (Zhang, Yang, Tang, Chen, & You, 2015) with some modifications.

179 Approximately 1.6 g of each gel sample formed in a 2 mL screw-cap chromatogram

180 vial were placed inside a cylindrical glass tube (15 mm in diameter) and inserted into

181 the NMR probe of a Niumag Benchtop Pulsed NMR analyser (Niumag PQ001; Niumag

182 Electric Corporation, Shanghai, China). The analyser was operated at 32 ℃ and a

183 resonance frequency of 18 MHz. The T_2 was measured using the Carr-Purcell-

184 Meiboom-Gill sequence with 4 scans, 8000 echoes, 2.0 s between scans, and 400 µs

185 between pulses of 90° and 180°. The T_2 relaxation curves were fitted to a multi-

186 exponential curve with the MultiExp Inv Analysis software (Niumag Electric

187 Corporation, Shanghai, China), which used the inverse Laplace transform algorithm.

188 *2.10. SPME–GC/MS*

189 A stock solution containing all selected flavours (aldehydes and ketones) was freshly

190 prepared in methanol (HPLC grade) and sealed in brown gas-tight glass bottles to

191 prevent volatilising. The stock solution was then pipetted to control and oxidised MP

192 suspensions (30 mg/mL), to a final concentration of 1 mg/kg for each flavour. Each

193 mixture (8 mL protein/control solution + 50 µL stock solution) was placed in a 20-mL

194 headspace vial and sealed with a polytetrafluoroethylene (PTFE)-faced silicone septum

195 (Supelco, Bellefonte, PA, USA). For gelation, the control and oxidised MP gels were

196 developed according to *Section 2.9.1*. The gel vials were stored at 25 °C for 16 h to

197 allow equilibration.

198 The quantities of flavour compounds present in the headspace of gel vials were

199 determined using solid-phase microextraction (SPME) followed by gas

200 chromatography/mass spectroscopy (GC/MS) analysis according to the procedure

201 described by Zhou et al. (2014a). The SPME parameters were as follows: 75 μm

202 Carboxen/polydimethylsiloxane (CAR/PDMS) fibre (Supelco, Bellefonte, PA),

203 equilibrated at 45°C for 20 min, extracted at 45°C for 30 min, desorbed at 220°C for 5

204 min. GC-MS conditions: TR-Wax column (30 m × 0.32 mm× 0.25 μm; J&W Scientific,

205 Folsom, CA, USA) was used for separation. The carrier gas was high purity helium at

206 a linear flow rate of 20.4 cm s^{-1}. The initial GC oven temperature was 38°C, held for 6

207 min, rising to 105°C at a rate of 6°C min^{-1}, then raised to 220°C at a rate of 15°C min$^-$

208 ^{1}, and held at 220°C for 5 min. The mass spectrometry conditions were electron

209 ionisation (EI) at 70 eV, electron multiplier voltage 350 V, scanning speed 3.00 scans/s,

210 mass range m/z 33–350. The results were expressed as the difference in peak areas of

211 flavour compounds between the oxidised MP gels and the control gel, calculated by the

212 following equation (2):

213   Free flavour compound (%) = (peak area protein/peak area control) × 100   (2)

214 *2.11. Statistical analysis*

215   Data were expressed as means ± standard deviations of triplicate determinations.

216 Statistical calculation was investigated by analysis of variance using SPSS 17.0 (SPSS,

217 Inc., Chicago, IL). The means were compared using Duncan's multiple range test ($p <$

218 0.05).

219

220 **3. Results and discussion**

221 *3.1. Total and reactive SH groups, surface hydrophobicity, salt solubility and turbidity*

222   The loss of SH groups is one of the primary common characteristics of protein

223 changes under oxidative attack (Xiong et al., 2009). As presented in **Table 1**, compared

224 with the control, the total and reactive SH contents both decreased continuously upon

225 oxidation with the increase of H_2O_2 concentrations ($p < 0.05$). MP are rich in SH groups

226 that can be readily converted to disulphide linkages (S–S) upon oxidative stress (Cao,

227 True, Chen, & Xiong, 2016). The decrease in total and reactive SH contents signified

228 that the SH groups of cysteine were oxidised with the formation of S–S (Sante-

229   Lhoutellier, Aubry, & Gatellier, 2007). Cao et al. (2018) also suggested that SH groups

230   in G-actin were susceptible to hydroxyl radicals and easily changed into intermolecular

231   S–S. Hence, the generated hydroxyl radicals (0.05–5.0 mM H_2O_2) were responsible for

232   the decrease in total and reactive SH contents. In addition, contents of total and reactive

233   SH also significantly decreased ($p < 0.05$) in 0 mM H_2O_2 compared with the control,

234   which may be associated with oxidation induced by Fe^{3+} (Fe^{3+} catalyses H_2O_2 to

235   produce hydroxyl radicals).

236   For monitoring the subtle changes in physical and chemical states of proteins, surface

237   hydrophobicity is a suitable parameter (Sante-Lhoutellier et al., 2007). As shown in

238   **Table 1**, compared with the control, the hydrophobicity of MP (0 mM H_2O_2)

239   significantly increased ($p < 0.05$), implying that the addition of ascorbic acid, Fe^{3+} and

240   oxidative terminators may markedly increase the protein surface hydrophobicity. In

241   addition, surface hydrophobicity of MP gradually increased with the increase of H_2O_2

242   concentrations (0.05–5.0 mM), and the results were similar to those of some previous

243   reports (Cao et al., 2018; Sun et al., 2013). Chelh et al. (2006) suggested that the

244   increase of surface hydrophobicity could be attributed to the unfolding of MP, thus

245   exposing previously buried nonpolar amino acids at their surface. Oxidative damage

246   could induce partial unfolding of MP, thereby exposing the hydrophobic amino acids

247   that were normally buried in protein molecules (Estévez, 2011; Sante-Lhoutellier et al.,

248   2007). Moreover, the cleavage of certain peptides under oxidative stress may also result

249   in the enhancement of surface hydrophobicity (Pacifici, 1987).

250   Salt solubility can reflect the extent of proteins aggregation (Shen et al., 2019). As

251   shown in **Table 1**, compared with the control, salt solubility of MP revealed a slight

252   increase (1.19–3.43%; $p < 0.05$) with low concentrations of oxidant (0–0.2 mM), and

253   then exhibited a rapid decrease (0.59–51.36%; $p < 0.05$) for the further oxidant

254 treatments (0.5–5.0 mM). A slight oxidation could cause a subtle unfolding of proteins

255 (Estévez, 2011), which may lead to better solubility in the salt solution. Nevertheless,

256 with further increase in oxidant, the solubility of MP drastically decreased due to the

257 stronger oxidative attack. This could be explained by the enhancement of surface

258 hydrophobicity and the excessive protein aggregates (Sun, Li, Zhou, Zhao, & Zhao,

259 2014). The exposure of hydrophobic patches or individual groups, aggregation and

260 polymerisation through S–S are all associated with the solubility decrease (Li, Xiong,

261 & Chen, 2012).

262   Turbidity is attributed to the presence of protein aggregates. The turbidity of MP

263 suspensions (**Table 1**) increased ($p < 0.05$) with the increased addition of H_2O_2 (0–5.0

264 mM), which accorded with the loss of SH and the increase of surface hydrophobicity.

265 This indicated that the oxidised incubation could obviously enhance the aggregation

266 behaviour of proteins. Under further analysis, this phenomenon was noted to be caused

267 by the increased surface hydrophobicity due to the exposure of interior hydrophobic

268 amino acid residues and the formation of intra- and intermolecular cross-links under

269 oxidative attack (Li et al., 2012), thus leading to the turbidity increase of MP

270 suspensions.

271 *3.2. Particle size distributions*

272   Particle size distributions can be used to monitor the aggregation behaviours of

273 proteins under oxidative attack. As shown in **Fig. S1**, compared with the control, the

274 particle size distribution of MP exhibited an obvious shift towards larger particles with

275 the increase of H_2O_2 concentrations. Protein oxidation could promote intermolecular

276 aggregation behaviours between protein molecules, thus increasing the particle size

277 values (Xiong et al., 2009). Specifically, the $D_{3,2}$ value of MP after oxidation showed

278 no significant difference ($p > 0.05$), while the values for other particle sizes ($D_{4,3}$ and

279     $D_{v,0.5}$) (**Table 2**) increased significantly ($p < 0.05$). The large droplets or droplet

280   aggregates have higher weight in the calculation of the $D_{4,3}$ value than they do in the

281   calculation of the $D_{3,2}$ value, and samples with similar $D_{3,2}$, but different $D_{4,3}$ would

282   result primarily from the amount of large droplets or droplet aggregates (Sun et al.

283   2014). This indicates that protein aggregation occurred after oxidation. Moreover, the

284   SH, surface hydrophobicity and turbidity analysis (**Table 1**) conformed to the

285   enhancement of association behaviours between protein molecules with the increase of

286   H_2O_2 concentrations, thereby enlarging the diameter of particles.

287   *3.3. SDS-PAGE*

288   The aggregation behaviours of the control and oxidised MP were further studied

289   using SDS-PAGE analysis (**Fig. S2**). In the absence of dithiothreitol, a large polymer

290   appeared at the top of the stack gel (**Fig. S2A**), suggesting the aggregation of MP. In

291   addition, MP aggregates induced by oxidative attack could form much larger aggregates

292   that could not enter the gel. Moreover, the intensities of the aggregation bands and the

293   aggregates all decreased and were not recovered in the presence of dithiothreitol (**Fig.**

294   **S2B**). This phenomenon indicated that the cross-links of the MP induced by oxidation

295   were not only through S–S but also through other covalent bonds (Cao et al., 2016). As

296   shown in the comparison between **Fig. S2A** and **Fig. S2B**, myosin heavy chain (MHC),

297   α-actinin and actin participated in the formation of aggregates.

298   *3.4. Gel properties*

299   *3.4.1. Hardness and WHC*

300   As aforementioned, oxidation had a pronounced effect on the physicochemical states

301   of MP. The hardness (**Fig. 1A**) and WHC (**Fig. 1B**) of the control and oxidised MP gels

302   were further evaluated. The mean hardness of the control gel was 21.9 ± 1.4 g and this

303   value was similar to that found by Xu, Han, Fei, and Zhou (2011). Compared with the

304   control, the hardness of mildly oxidised MP gels (0–0.2 mM H_2O_2) increased

305   significantly ($p < 0.05$). Due to the slightly unfolding of MP (salt solubility analysis), a

306   firmer matrix structure of MP gels may be formed during the heating process. Xiong et

307   al. (2010) also suggested that mild oxidation could promote protein network formation

308   and enhance the gelation of MP. Nevertheless, with more addition of H_2O_2 (0.5–5.0

309   mM), a significant decrease ($p < 0.05$) in gel hardness was observed, implying a weak

310   gel structure. In particular, heat-induced S–S bonds were regarded as an important

311   supporting force for the matrix structure of protein gels (Xiong et al., 2010). Hence, the

312   decrease of hardness may be attributed to the reduction of SH contents in MP (**Table

313   1**), thus leading to disordered aggregation replacing the ordered cross-links during

314   heating. Moreover, the decrease of salt solubility of MP could limit the ordered cross-

315   links within protein molecules during gelation.

316   Furthermore, WHC gave a quantitative indication of the amount of water maintained

317   within the protein gel structure, and this could reflect aspects of the spatial structure of

318   the gel (Zhou et al., 2014b). As shown in **Fig. 1B**, the control gel had the strongest

319   ability to retain water, and the WHC abilities of oxidised MP gels were gradually

320   weakened ($p < 0.05$) with an increase of H_2O_2 concentration (0–5.0 mM). As reported,

321   the structural integrity of myosin is of paramount importance for gelation and water

322   holding in meat (Deng et al., 2010). Oxidative damage to myosin could result in an

323   inferior gel network formation, causing lower elasticity with poor WHC in the gel

324   matrix. This was in good agreement with the surface hydrophobicity of MP (**Table 1**),

325   which could also reflect the affinity of proteins with water.

326   *3.4.2. Microstructure*

327   The changes in MP gel properties induced by oxidation were further investigated by

328   the measurements of surface morphologies, and the results are presented in **Fig. 2**. The

control gel appeared as a flat surface with several visible pores (**Fig. 2A** and **2B**), which

indicated an ordered network structure due to protein stretching. At 2000 times

magnification, the protein (control gel) exhibits a good cross-linked structure.

Compared to the control, the mildly oxidised MP gels (0–0.2 mM H_2O_2) exhibited some

fragments on the gel surface and a lower number of visible pores (**Fig. 2B**). The pore

size of these gel was significantly reduced ($\times$ 500), and the original cross-linked

structure was transformed into an aggregated particle structure, and the roughness is

increased ($\times$ 2000), thereby yielding a firm pattern (hardness analysis). This

phenomenon was attributed to the slight shrinkage of MP upon oxidation (Astruc,

Gatellier, Labas, Lhoutellier, & Marinova, 2010). As a continuous increase of H_2O_2

(0.5–1.0 mM), aggregated particles and roughness further increased with the much

more smaller pore size. Under 5 mM H_2O_2, the pores disappeared, and the fragments

aggregated into clump structures. The surface morphologies of these gels revealed an

uneven dense structure with aggregates and increased the roughness of the overlapped

surface. This trend was in accordance with a previous observation (Zhou et al., 2014a).

Formation of the surface structures of oxidised MP gels described previously could be

attributed to the intra- and intermolecular cross-links and aggregates within proteins

induced by oxiditive modification (Sun et al., 2014), thus leading to a disordered gel

network structure during the heating process. In addition, the clump structures clearly

aggregated into larger globular clusters when subjected to higher oxidative attack (2.5–

5.0 mM H_2O_2), indicating an accelerated state of aggregation (**Fig. 2B**). These structural

features implied that proteins under higher oxidative stress could undergo more steric

modifications and contribute to the layered surface with bunched aggregation (Zhou et

al., 2014a). These micrographs demonstrated the significant influences of oxidative

treatments on protein gels. Moreover, these observations were in agreement with the

354   results of SH contents, surface hydrophobicity, turbidity and particle size distributions

355   (**Table 1** and **Fig. S1**).

356   *3.4.3. Relaxation time analysis*

357   A fitted T_2 distribution was used to assess the relaxation time of hydrogen protons.

358   The T_2 relaxation time distributions for the control and oxidised MP gels are shown in

359   **Fig. 3**. Three peaks were noted for the control and in the gels with lower H_2O_2

360   concentrations (0–1.0 mM), while four peaks were noted for the gels with 2.5–5.0 mM

361   H_2O_2. This meant that the protein gels under different oxidation levels could restrict

362   water mobility at different magnitudes (Wang, Zhang, Bhandari, & Gao, 2016). The

363   components with shorter relaxation time, T_{2b} and T_{21} (0–10 ms), represented the protons

364   in macromolecular structures and those combined closely with the macromolecular

365   structures, respectively. The component T_{22} (10–100 ms) was assigned to myofibrillar

366   water and water within the protein structure. The last peak represented the extra-

367   myofibrillar water (T_{23}) population, and this peak appeared between 300 and 2000 ms.

368   Generally, the existence of four groups of water in MP gels was in agreement with some

369   previous reports (Wang et al., 2016; Zheng et al., 2015).

370   With oxidation treatments, the relaxation time of T_{22} increased from 14.17 ms

371   (control gel) to 16.30–28.48 ms (oxidised gels) with increasing H_2O_2 concentrations,

372   and T_{23} increased from 613.59 ms (control and oxidised gels with 0–1.0 mM H_2O_2) to

373   705.48 ms (oxidised gels with 2.5–5.0 mM H_2O_2) (**Table 1S**). If the relaxation time is

374   shorter, a smaller amount of mobile water is available, whereas the longer relaxation

375   time implies a more mobile water fraction (Shao et al., 2016). Hence, the increased T_2

376   relaxation times suggested that oxiditive modifications could lead to a certain level of

377   the immobilised water shifting to free water. This may be associated with the

378   enhancement in hydrophobic trend arising from the increased surface hydrophobicity

379 of MP (**Table 1**). Also, the increased aggregation behaviours (**Fig. S1** and **Table 2**)

380 within MP molecules could decrease the surface areas in gels, thus resulting in a

381 decrease of macromolecule sites for WHC (Wang et al., 2016). Moreover, the relaxation

382 component T_{2b} had divided into another part (T_{21}) at higher H_2O_2 concentrations (2.5–

383 5.0 mM). This may be due to the degradation of MP upon higher oxidative stress, thus

384 contributing to greater mobility of the water in macromolecular structures. In addition,

385 McDonnell et al. (2013) suggested that certain side-chains, such as carboxyl-, amino-,

386 hydroxyl-, sulfhydryl-groups, and even carbonyl- and imido-groups, in proteins were

387 responsible for water binding. Therefore, the changes in T_{2b} relaxation time

388 corresponded to the availability of protein side-chains, as related to the oxidative

389 modifications. These phenomena accorded with the WHC results (**Fig. 1B**).

390 *3.5. Binding of MP gels to flavours*

391 A homologous series of aldehydes and ketones that varied in chain length was

392 selected to investigate the binding performances of MP gels under different oxidation

393 levels. In protein solution systems, the longer the carbon chain, the stronger the ability

394 of the flavour compound to bind to the protein. (Lou, Yang, Sun, Pan, & Cao, 2017;

395 Zhou et al., 2014a). By contrast, in this study, the free percentages of aldehydes and

396 ketones in each vial increased with the increase in carbon chain length (**Fig. 4**),

397 suggesting it was more difficult for the flavour compounds with longer chain length to

398 bind with MP gels, which can be related to the steric effect of the gel network structure.

399 In addition, consistent with the finding reported by Wang and Arntfield (2015), the free

400 percentage of all aldehydes was lower than that of the ketones with the same carbon

401 numbers in all vials (**Fig. 4**), suggesting that the binding abilities of oxidised MP gels

402 to aldehydes were stronger than to ketones. This was because of the higher molecular

403　activities and lower steric hindrance effects of carbonyl groups in aldehydes (Kühn et

404　al., 2008).

405　　As shown in Fig. 4A, the free percentages of hexanal and heptanal first decreased

406　and then increased significantly ($p < 0.05$) with increased oxidation levels (0–5.0 mM).

407　Although the free percentages of pentanal and octanal showed no significant changes

408　($p > 0.05$) at different oxidation levels, their trends were similar to those of hexanal and

409　heptanal. The free percentages of ketones (Fig. 4B) (except for 2-octanone) showed no

410　significant changes at different oxidation levels (0–5.0 mM). Volatile release from food

411　is primarily controlled by the following two factors: the nature of aroma compounds

412　(such as volatility and polarity) and the resistance to mass transfer from a food matrix

413　to the air phase (Mao, Roots, & Miao, 2015). Protein oxidation increased the surface

414　hydrophobicity and interaction of proteins (**Table 1**); the oxidised MP gels could

415　exhibit higher binding phenomena through stronger interaction force (such as

416　hydrophobic interaction) to flavours, thus reducing their free percentages in the

417　headspace. However, the binding of a certain protein gel to flavours may also be

418　influenced by the steric hindrance effect or mass transfer from MP gel. Therefore,

419　flavours with a longer carbon chain could produce a stronger steric hindrance effect due

420　to the gel network, thus preventing their access to the interior hydrophobic binding sites

421　and thus increasing their presence in the headspace (Wang & Arntfield, 2015). As

422　shown in **Fig. 2**, as the degree of oxidation increased, the homogeneous cross-linked

423　MP gel network gradually changes to a granular shape, and gradually loses the gel

424　network structure (the pore size of the gel network also gradually decreases), which

425　increases the steric resistance of the MP gel, increasing the content of aroma

426　components in the headspace vial. Therefore, the release of flavour compounds

427 depended on the balance between protein–flavour compound interactions and gel

428 network–flavour compound limitations (Mao et al., 2014).

429 **4. Conclusions**

430 The influence of oxidative modifications induced by H_2O_2 (0–5.0 mM) on the

431 properties of MP and MP gels was investigated. With an increase in H_2O_2

432 concentrations, MP tended to expose their interior hydrophobic amino acids and to lose

433 SH content, thus leading to enhanced aggregation behaviours, an increase in surface

434 hydrophobicity and turbidity and a larger particle size distribution. The covalent bonds

435 in the MP aggregates included S–S, among others. Under oxidative attack, MP gels

436 demonstrated decreased WHC and more mobility of water. Mild oxidation (0–0.5 mM

437 H_2O_2) slightly increased the salt solubility of MP and the hardness of MP gels. The

438 abilities of MP gels to bind to aldehydes and ketones decreased with the growth of the

439 carbon chain. The release of flavours in a gel was different from that in a protein

440 solution due to mass transfer from a gel matrix to the air phase and heat treatment.

441 Under the balance between protein–flavour compound interaction and gel network–

442 flavour compound steric hindrance, MP oxidation only significantly affected ($p < 0.05$)

443 the binding between MP gels and hexanal, heptanal, and 2-octanone, while other

444 flavour compounds were not affected significantly ($p > 0.05$).

445

452

References

453

454 Astruc, T., Gatellier, P., Labas, R., Lhoutellier, V. S., & Marinova, P. (2010).

455   Microstructural changes in *m. rectus abdominis* bovine muscle after heating. *Meat*

456   *Science, 85*(4), 743–751.

457 Boland, A. B., Delahunty, C. M., & van Ruth, S. M. (2006). Influence of the texture of

458   gelatin gels and pectin gels on strawberry flavour release and perception. *Food*

459   *Chemistry, 96*(3), 452–460.

460 Cao, Y., True, A. D., Chen, J., & Xiong, Y. L. (2016). Dual Role (Anti- and Pro-oxidant)

461   of Gallic Acid in Mediating Myofibrillar Protein Gelation and Gel *in Vitro*

462   Digestion. *Journal of Agricultural and Food Chemistry, 64*(15), 3054–3061.

463 Chelh, I., Gatellier, P., & Santé-Lhoutellier, V. (2006). Technical note: A simplified

464   procedure for myofibril hydrophobicity determination. *Meat Science, 74*(4), 681–

465   683.

466 Deng, Y., Rosenvold, K., Karlsson, A. H., Horn, P., Hedegaard, J., Steffensen, C. L.,

467   & Andersen, H. J. (2010). Relationship Between Thermal Denaturation of Porcine

468   Muscle Proteins and Water-holding Capacity. *Journal of Food Science, 67*(5),

469   1642–1647.

470 Estévez, M. (2011). Protein carbonyls in meat systems: A review. *Meat Science, 89*(3),

471   259–279.

472 Gierczynski, I., Guichard, E., & Laboure, H. (2011). Aroma perception in dairy

473   products: the roles of texture, aroma release and consumer physiology. A

474   review. *Flavour and Fragrance Journal*, *26*(3), 141–152.

475 Guichard, E. (2002). Interactions between flavor compounds and food ingredients and

476   their influence on flavor perception. *Food Reviews International, 18*(1), 49–70.

477   Guinard, J. X., & Marty, C. (1995). Time‑intensity measurement of flavor release from

478   a model gel system: effect of gelling agent type and concentration. *Journal of Food*

479   *Science*, *60*(4), 727–730.

480   Hansson, A., Giannouli, P., & van Ruth, S. (2003). The influence of gel strength on

481   aroma release from pectin gels in a model mouth and *in vivo*, monitored with

482   proton-transfer-reaction mass spectrometry. *Journal of Agricultural and Food*

483   *Chemistry*, *51*(16), 4732–4740.

484   Juteau-Vigier, A., Atlan, S., Deleris, I., Guichard, E., Souchon, I., & Trelea, I. C. (2007).

485   Ethyl hexanoate transfer modeling in carrageenan matrices for determination of

486   diffusion   and   partition   properties. *Journal   of   Agricultural   and   Food*

487   *Chemistry, 55*(9), 3577–3584.

488   Kühn, J., Considine, T., & Singh, H. (2008). Binding of flavor compounds and whey

489   protein isolate as affected by heat and high pressure treatments. *Journal of*

490   *Agricultural and Food Chemistry, 56*(21), 10218–10224.

491   Lee, H. A., Choi, S. J., & Moon, T. W. (2006). Characteristics of sodium caseinate- and

492   soy protein isolate-stabilized emulsion-gels formed by microbial transglutaminase.

493   *Journal of Food Science, 71*(6), C352–C357.

494   Li, C., Xiong, Y. L., & Chen, J. (2012). Oxidation-induced unfolding facilitates Myosin

495   cross-linking in myofibrillar protein by microbial transglutaminase. *Journal of*

496   *Agricultural & Food Chemistry, 60*(32), 8020–8027.

497   Lou, X., Yang, Q., Sun, Y., Pan, D., & Cao, J. (2017). The effect of microwave on the

498   interaction   of   flavour   compounds   with   G-actin   from   grass   carp

499   (Catenopharyngodon idella). *Journal of the Science of Food and Agriculture,*

500   *97*(12), 3917–3922.

501   Mao, L., Roos, Y. H., & Miao, S. (2014). Study on the rheological properties and

502   volatile release of cold-set emulsion-filled protein gels. *Journal of Agricultural*

503   *and Food Chemistry, 62*(47), 11420–11428.

504   Mao, L., Roos, Y. H., & Miao, S. (2015). Effect of maltodextrins on the stability and

505   release of volatile compounds of oil-in-water emulsions subjected to freeze–thaw

506   treatment. *Food Hydrocolloids, 50*, 219–227.

507   McDonnell, C. K., Allen, P., Duggan, E., Arimi, J. M., Casey, E., Duane, G., & Lyng,

508   J. G. (2013). The effect of salt and fibre direction on water dynamics, distribution

509   and mobility in pork muscle: a low field NMR study. *Meat Science, 95*(1), 51–58.

510   O'Neill, T. E., & Kinsella, J. E. (1987). Binding of alkanone flavors to β-lactoglobulin:

511   effects of conformational and chemical modification. *Journal of Agricultural and*

512   *Food Chemistry, 35*(5), 770–774.

513   Pacifici, R. E. (1987). Protein damage and degradation by oxygen radicals. *Journal of*

514   *Biological Chemistry, 262*(20), 9902–9907.

515   Sante-Lhoutellier, V., Aubry, L., & Gatellier, P. (2007). Effect of oxidation on *in vitro*

516   digestibility of skeletal muscle myofibrillar proteins. *Journal of Agricultural &*

517   *Food Chemistry, 55*(13), 5343–5348.

518   Shao, J. H., Deng, Y. M., Song, L., Batur, A., Jia, N., & Liu, D. Y. (2016). Investigation

519   the effects of protein hydration states on the mobility water and fat in meat batters

520   by LF-NMR technique. *LWT - Food Science and Technology, 66*, 1–6.

521   Shen, H., Zhao, M., & Sun, W. (2019). Effect of pH on the interaction of porcine

522   myofibrillar proteins with pyrazine compounds. *Food Chemistry, 287*, 93–99.

523   Sun, W., Li, Q., Zhou, F., Zhao, H., & Zhao, M. (2014). Surface characterization of

524   oxidized myofibrils using X-ray photoelectron spectroscopy and scanning electron

525   microscopy. *Journal of Agricultural & Food Chemistry, 62*(30), 7507–7514.

526 Sun, W., Zhou, F., Sun, D.-W., & Zhao, M. (2013). Effect of Oxidation on the

527 Emulsifying Properties of Myofibrillar Proteins. *Food and Bioprocess Technology,*

528 *6*(7), 1703–1712.

529 Wang, K., & Arntfield, S. D. (2015). Binding of selected volatile flavour mixture to

530 salt-extracted canola and pea proteins and effect of heat treatment on flavour

531 binding. *Food Hydrocolloids, 43*, 410–417.

532 Wang, K., & Arntfield, S. D. (2016). Modification of interactions between selected

533 volatile flavour compounds and salt-extracted pea protein isolates using chemical

534 and enzymatic approaches. *Food Hydrocolloids, 61*, 567–577.

535 Wang, L., Zhang, M., Bhandari, B., & Gao, Z. (2016). Effects of malondialdehyde-

536 induced protein modification on water functionality and physicochemical state of

537 fish myofibrillar protein gel. *Food Research International, 86*, 131–139.

538 Xia, X., Kong, B., Xiong, Y., & Ren, Y. (2010). Decreased gelling and emulsifying

539 properties of myofibrillar protein from repeatedly frozen-thawed porcine

540 longissimus muscle are due to protein denaturation and susceptibility to

541 aggregation. *Meat Science, 85*(3), 481–486.

542 Xiong, Y., Blanchard, S. P., Ooizumi, T., & Ma, Y. (2010). Hydroxyl radical and ferryl-

543 generating systems promote gel network formation of myofibrillar protein.

544 *Journal of Food Science, 75*(2), C215–C221.

545 Xiong, Y. L., Park, D. K., & Ooizumi, T. (2009). Variation in the cross-linking pattern

546 of porcine myofibrillar protein exposed to three oxidative environments. *Journal*

547 *of Agricultural & Food Chemistry, 57*(1), 153–159.

548 Xu, X. L., Han, M. Y., Fei, Y., & Zhou, G. H. (2011). Raman spectroscopic study of

549 heat-induced gelation of pork myofibrillar proteins and its relationship with

550 textural characteristic. *Meat Science, 87*(3), 159–164.

551 Zhang, Z., Yang, Y., Tang, X., Chen, Y., & You, Y. (2015). Chemical forces and water

552   holding capacity study of heat-induced myofibrillar protein gel as affected by high

553   pressure. *Food Chemistry, 188*, 111–118.

554 Zheng, H., Xiong, G., Han, M., Deng, S., Xu, X., & Zhou, G. (2015). High

555   pressure/thermal combinations on texture and water holding capacity of chicken

556   batters. *Innovative Food Science & Emerging Technologies, 30*, 8–14.

557 Zhou, F., Zhao, M., Su, G., & Sun, W. (2014b). Binding of aroma compounds with

558   myofibrillar proteins modified by a hydroxyl-radical-induced oxidative system.

559   *Journal of Agricultural & Food Chemistry, 62*(39), 9544–9552.

560 Zhou, F., Zhao, M., Zhao, H., Sun, W., & Cui, C. (2014a). Effects of oxidative

561   modification on gel properties of isolated porcine myofibrillar protein by peroxyl

562   radicals. *Meat Science, 96*(4), 1432–1439.

563 **Table 1** Total and reactive sulfhydryl groups, surface hydrophobicity, salt solubility and turbidity of the control and oxidised MP

H_2O_2 (mM)	Total sulfhydryl (nmol/mg protein)	Reactive sulfhydryl (nmol/mg protein)	Surface hydrophobicity (μg BPB)	Salt solubility (%)	Turbidity (FTU)
Control	9.02 ± 0.12g	8.45 ± 0.09h	22.75 ± 1.22a	83.57 ± 1.39d	83.11 ± 0.82a
0.0	8.30 ± 0.04f	6.35 ± 0.05g	38.02 ± 0.86bc	84.57 ± 0.46de	84.27 ± 0.58a
0.05	8.19 ± 0.02f	5.99 ± 0.07f	36.57 ± 2.15b	86.43 ± 1.09e	87.13 ± 0.56b
0.2	7.99 ± 0.05e	5.56 ± 0.11e	38.59 ± 0.85c	86.39 ± 0.66e	90.44 ± 2.37c
0.5	6.95 ± 0.03d	3.24 ± 0.11d	41.26 ± 0.72d	83.08 ± 0.94d	91.71 ± 1.99c
1.0	5.87 ± 0.03c	2.84 ± 0.07c	42.47 ± 0.34d	79.28 ± 2.73c	92.74 ± 0.91c
2.5	3.52 ± 0.11b	1.82 ± 0.05b	46.23 ± 0.71e	52.23 ± 0.96b	97.05 ± 1.47d
5.0	1.01 ± 0.05a	0.37 ± 0.03a	49.88 ± 1.08f	40.65 ± 1.02a	96.70 ± 0.90d

564 Values in the same column with different letters were significantly different ($p < 0.05$).

565   **Table 2** Average particle size ($D_{3,2}$ and $D_{4,3}$) and span of the control and oxidised MP

H_2O_2 (mM)	$D_{3,2}$ (µm)	$D_{4,3}$ (µm)	$D_{v,0.5}$ (µm)	Span
Control	41.55 ± 1.51a	99.58 ± 2.76a	69.57 ± 1.63a	2.89 ± 0.05ab
0.0	50.93 ± 0.84b	119.53 ± 1.09b	86.79 ± 1.30b	2.80 ± 0.09a
0.05	51.47 ± 1.80b	120.12 ± 3.39bc	86.18 ± 3.36b	2.84 ± 0.06a
0.2	51.06 ± 1.58b	121.22 ± 3.70bc	87.00 ± 3.40b	2.86 ± 0.03a
0.5	51.53 ± 1.19b	125.19 ± 2.46bc	87.57 ± 2.03b	3.01 ± 0.03bc
1.0	48.80 ± 1.90b	126.49 ± 4.66c	87.62 ± 3.70b	3.11 ± 0.03cd
2.5	50.72 ± 2.12b	138.31 ± 4.05d	96.93 ± 3.48c	3.12 ± 0.06cd
5.0	51.77 ± 2.21b	146.12 ± 5.07e	101.82 ± 4.95c	3.18 ± 0.17d

566   Values in the same column with different letters were significantly different ($p < 0.05$).

Figure Captions:

Fig. 1. Hardness (A) and WHC (B) of the control and oxidised MP gels. Different letters

denote a significant difference between means ($p < 0.05$).

Fig. 2. Scanning electron microscope micrographs at $\times 500$ (A) and $\times 2000$ (B)

magnification of the control and oxidised MP gels. Scale bars indicate 100 μm (A) and

20 μm (B).

Fig. 3. Distributions of T_2 relaxation times of the control and oxidised MP gels.

Fig. 4. Binding phenomena of the control and oxidised MP gels to selected aldehydes

(A) and ketones (B). Results were expressed as percentage of free flavours found in the

headspace of the control gel. Capital letters denote significant differences ($p < 0.05$) in

flavour compound release for a same oxidant concentration, while lowercase letters

denote significant differences ($p < 0.05$) in compound release between oxidant

concentrations.

A

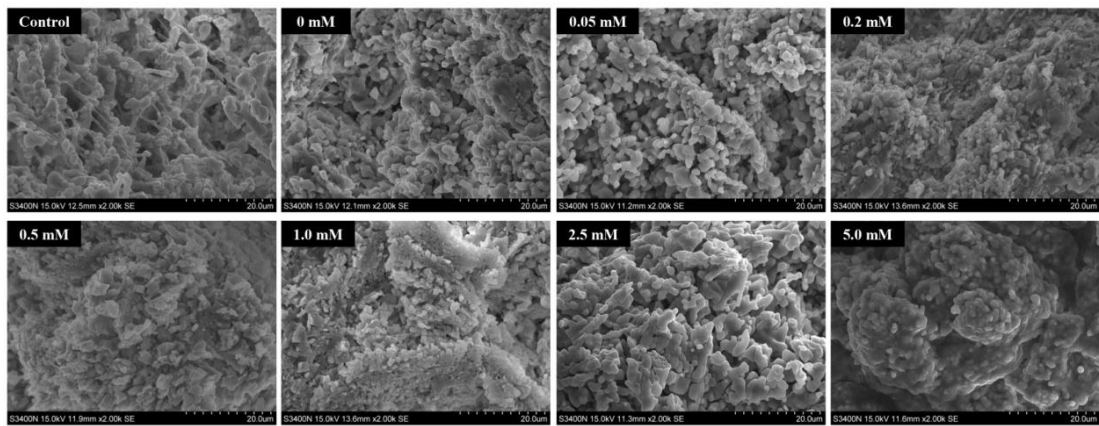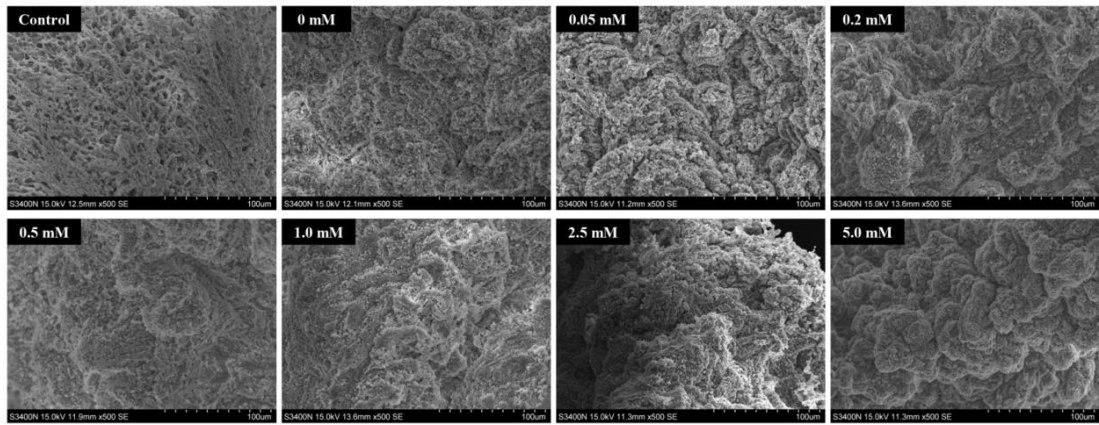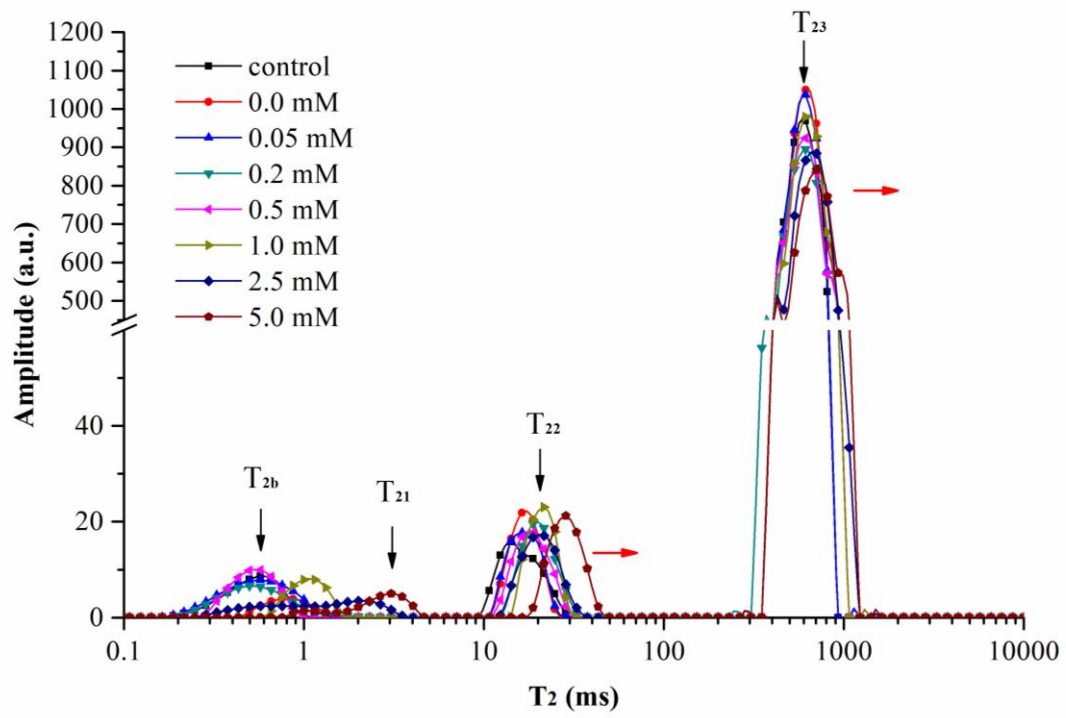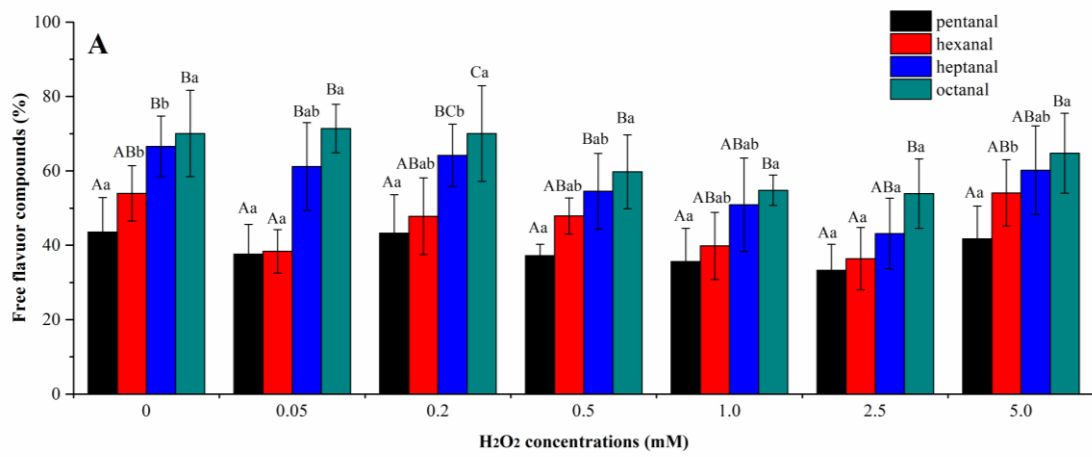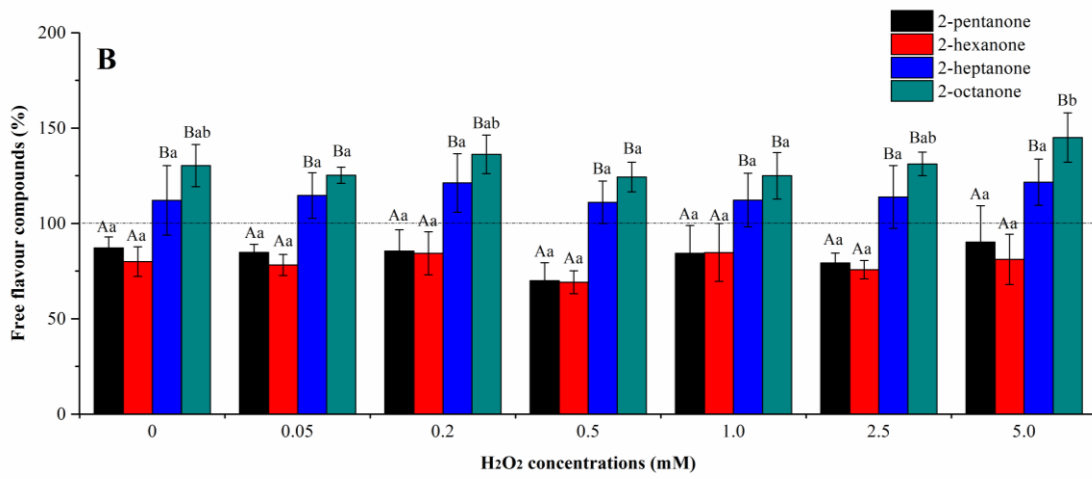580

B

581

582   **Fig. 1**

A

B
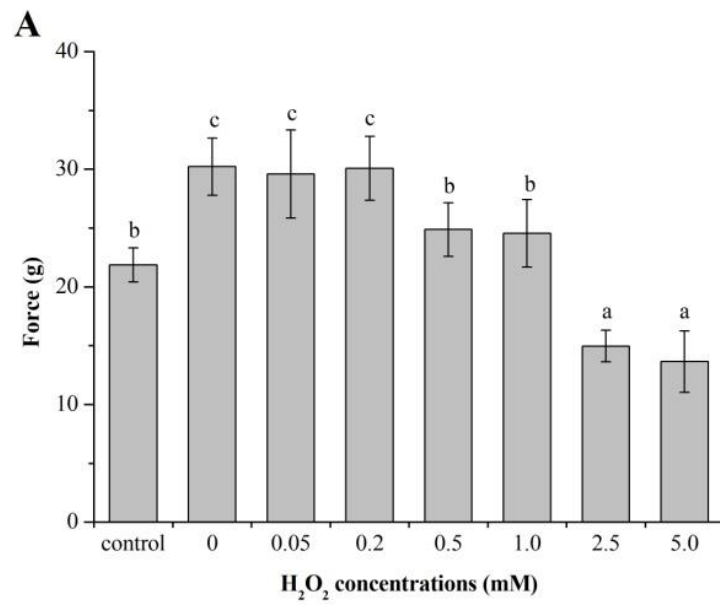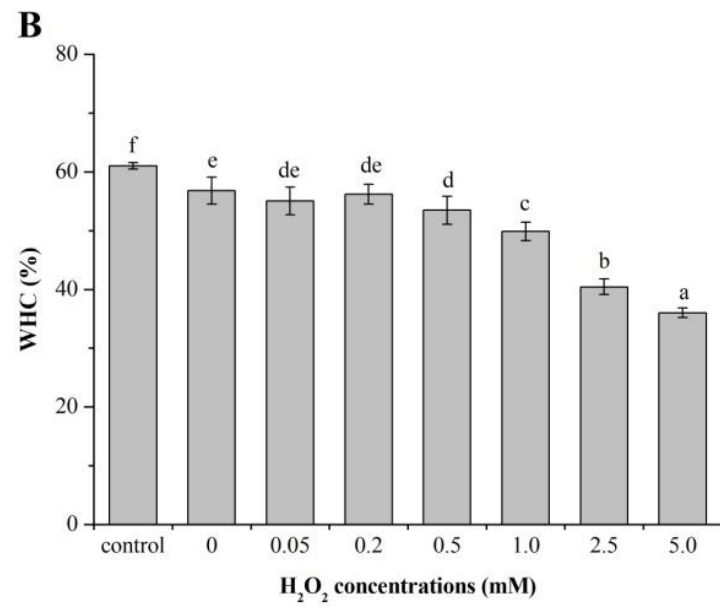
583

584 **Fig. 2**

585

586 **Fig. 3**

587

588

589   **Fig. 4**